



GLOBAL JOURNAL OF RESEARCHES IN ENGINEERING  
CIVIL AND STRUCTURAL ENGINEERING  
Volume 13 Issue 3 Version 1.0 Year 2013  
Type: Double Blind Peer Reviewed International Research Journal  
Publisher: Global Journals Inc. (USA)  
Online ISSN: 2249-4596 & Print ISSN: 0975-5861

# Determination of the Appropriate Plasticity Hardening Model for the Simulation of the Reverse Bending and Straightening of Wires for Civil Engineering Applications

By Kazeem K Adewole

*Newcastle University, United Kingdom*

**Abstract** - The industry requires an understanding of the effects of reverse bending and straightening test wires for civil engineering applications undergo to detect laminations in them on their tensile properties. In this paper, the identification of the appropriate plasticity hardening model for the simulation of wires reverse bending and straightening test which involves “double” strain reversal is presented. Finite element Simulations revealed that the isotropic hardening model predicted a continuous work hardening of the wire during the bending, reverse bending, and straightening operations and did not capture the softening of the wire due to the Bauschinger effect. Conversely, the combined hardening model adequately captured both the work hardening and Bauschinger effect that are associated with the reverse bending and straightening processes. Consequently, it is demonstrated that the combined hardening model is the appropriate plasticity hardening model for the simulation of reverse bending and straightening of carbon steel wires used for civil engineering applications. This paper thus established the appropriate plasticity hardening model required for the FE simulation of the wires’ reverse bending and straightening test Needed to investigate the effects of reverse bending and straightening test on the tensile and fracture properties of a typical wire used for civil engineering applications.

**Keywords** : *bauschinger effect, combined hardening, finite element simulation, isotropic hardening, laminations, reverse bending strain reversal wires.*

**GJRE Classification** : *FOR Code: 090599*



*Strictly as per the compliance and regulations of :*



# Determination of the Appropriate Plasticity Hardening Model for the Simulation of the Reverse Bending and Straightening of Wires for Civil Engineering Applications

Kazeem K Adewole

**Abstract** - The industry requires an understanding of the effects of reverse bending and straightening test wires for civil engineering applications undergo to detect laminations in them on their tensile properties. In this paper, the identification of the appropriate plasticity hardening model for the simulation of wires reverse bending and straightening test which involves "double" strain reversal is presented. Finite element simulations revealed that the isotropic hardening model predicted a continuous work hardening of the wire during the bending, reverse bending, and straightening operations and did not capture the softening of the wire due to the Bauschinger effect. Conversely, the combined hardening model adequately captured both the work hardening and Bauschinger effect that are associated with the reverse bending and straightening processes. Consequently, it is demonstrated that the combined hardening model is the appropriate plasticity hardening model for the simulation of reverse bending and straightening of carbon steel wires used for civil engineering applications. This paper thus established the appropriate plasticity hardening model required for the FE simulation of the wires' reverse bending and straightening test needed to investigate the effects of reverse bending and straightening test on the tensile and fracture properties of a typical wire used for civil engineering applications.

**Keywords** : bauschinger effect, combined hardening, finite element simulation, isotropic hardening, laminations, reverse bending, strain reversal, wires.

## 1. INTRODUCTION

Carbon steel wires are used in the construction of many civil engineering structures. Specifically, carbon steel wires are used as pre-stressing tendons and as suspension and/or cable-stayed bridge wires. Carbon steel wires are also incorporated into flexible pipes used for offshore oil and gas transportation as axial stress reinforcement. These wires are subject to a number of non-destructive tests to detect defects that could threaten their integrity in service. One of these tests is the reverse bending and straightening test which involves bending of the wire over the rotating left hand roller, reverse bending of the wire over the rotating middle roller and finally

**Author** : School of Chemical Engineering and Advanced Materials, Newcastle University, Newcastle upon Tyne, United Kingdom, NE1 7RU. E-mails : kkadewole@yahoo.com, k.k.adewole@ncl.ac.uk

straightening of the wire over the rotating right hand roller as shown in Figure 1 to detect laminations in the wires. A lamination is an elongated line-type defect or a long crack that is usually invisible and usually parallel to the surface of metal products (such as wires) produced through rolling or drawing process (Smith et al, 1957). It is essential to detect laminations in wires/bars used for civil engineering applications as the catastrophic rupture of pre-stressed concrete pipes has been attributed to the presence of long straight pre-service longitudinal cracks (i.e. laminations) in the pre-stressing wires used for pre-stressing the ruptured pre-stressed concrete pipes by the United States Bureau of Reclamation, 1994.

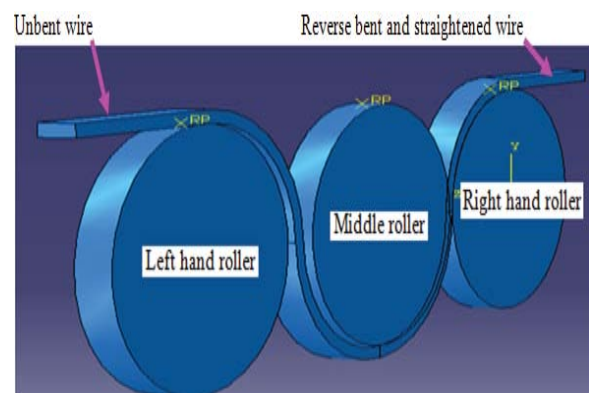


Figure 1 : Industrial reverse bending equipment with three rollers

In the current work, three dimensional FE simulations were conducted to identify the appropriate hardening model for the simulation of the wire reverse bending and straightening test. The FE simulation of the wire reverse bending and straightening test was conducted as a part of the research to investigate the effects of the combination of reverse bending and laminations on the tensile properties of a typical wire used for civil engineering applications. FE simulation was employed for the investigation of the effects of the combination of reverse bending and laminations on the tensile properties of the wire because it was not experimentally possible to simulate the long straight longitudinal cracks or laminations that are parallel to the

length of the wire specimens (such as the lamination found in the pre-stressing wires used to pre-stress the ruptured pre-stressed concrete pipe) using machining techniques. For an accurate simulation of the wires' reverse bending and straightening test, it is essential to employ an appropriate material constitutive model, particularly the plasticity hardening model that is able to capture the wires' behavior(s) during the various stages (bending, reverse bending and straightening) of the reverse bending and straightening test/process.

Most of the published literature on reverse bending of metal products (for example Firat (2007); Gau and Kinzel (2001)), are in sheet metal forming. The importance of using appropriate material constitutive model(s) in the finite element (FE) formability and springback predictions in sheet metal forming simulations has been emphasised by Gau and Kinzel (2001), Firat, (2007) and Taherizadeh et al, (2010). Material constitutive models that have been used in FE sheet metal forming predictions and springback analyses include the isotropic, kinematic and anisotropic hardening models. Combinations of two or more of these hardening models have also been used for FE sheet metal forming simulation and spring back prediction. Firat, (2007), Zhao and Lee, (1999), and Ken-ichiro, (2001) observed that the isotropic hardening model when used in reverse bending simulation overestimates the hardening component and does not predict the through-thickness stress distribution accurately because it does not consider the Bauschinger effect. The Bauschinger effect is responsible for the reduction in both the fatigue strength and the static yield strength of a metal when it is subjected to strain reversal (Takeda and Chen (1999). Zhao and Lee, (1999) reported that "the kinematic hardening rule underestimates the hardening component and exaggerates the Bauschinger effect". The shortcomings associated with using the isotropic and kinematic hardening models has led to an emerging new standard of models with mixed or combined hardening (a combination of two or more different hardening models) which has proven to increase the numerical reliability of sheet metal formability and springback predictions (Carbonnie et al, 2008).

An acceptable material model should be able to capture the many different material phenomena that occur during plastic deformation, such as work hardening and the Bauschinger effect, and should be able to provide the best possible fit to the actual material properties (Taherizadeh et al, 2010). Consequently, it is essential to understand the applicability of these models and their limitations in order to increase the accuracy of FE reverse bending simulations. To the best of the authors' knowledge, no guidance on the appropriate plasticity hardening model for the simulation of the reverse bending and straightening of a wire which involves "double" strain reversal (strain reversal due to

reverse bending and strain reversal due to straightening of the wires) has been published.

In this work, the three dimensional FE simulations were conducted using the isotropic elastic-plastic hardening model and the combined hardening plasticity models in-built in the Abaqus v 6.9.3 FE software materials library. The FE simulations with the isotropic and the combined hardening models were conducted in combination with the phenomenological shear damage and failure criterion. The details of the phenomenological shear failure model can be found in the work of Adewole and Bull, (2013). The details of the isotropic elastic-plastic and isotropic elastic-combined hardening plasticity models are presented in the following sections.

#### a) Isotropic Elastic-Plasticity Model

The isotropic elastic-plasticity model in Abaqus is based on a linear isotropic elasticity theory and a uniaxial-stress, plastic-strain strain-rate relationship (Simulia, 2007). The elastic aspect of the model is defined in terms of its volumetric and deviatoric components given in equations (1) and (2) respectively obtained from Simulia, (2007). The model is based on a von Mises yield surface with the yield function,  $f$ , given in equation (3) and a flow rule given in equation (4) obtained from (Simulia, 2007).

$$p = -K\varepsilon_{vol} \quad (1)$$

$$S = 2Ge^{el} \quad (2)$$

$$f = q = \sqrt{\frac{3}{2}}S : S \quad (3)$$

$$de^{pl} = \bar{d}e^{pl}n \quad (4)$$

Here  $p$  is the hydrostatic stress,  $\varepsilon_{vol}$  is the volume strain,  $S$  is the deviatoric stress,  $e^{el}$  is the deviatoric elastic strain,  $q$  is the von Mises equivalent stress,  $e^{pl}$  is the deviatoric plastic strain,  $\bar{e}^{pl}$  is the equivalent plastic strain,  $n = \frac{3}{2} \frac{S}{q}$ ,  $K$  is the bulk modulus and  $G$  is the shear modulus.  $K$  and  $G$  are calculated from the Young's modulus,  $E$ , and Poisson's ratio,  $\nu$ , of the material.

#### b) Isotropic Elastic-Combined Hardening Plasticity Model

The combined hardening model is a combination of the nonlinear kinematic and isotropic hardening models. The isotropic cyclic hardening component is based on the exponential law given in equation (5) obtained from Simulia, (2007). The kinematic hardening component is based on the

evolution of the backstress (a nonlinear evolution of the centre of the yield surface)  $\dot{\alpha}$  given in equation (6) obtained from Simulia, (2007).

$$\sigma^0 = Y_i + Q_\infty(1 - e^{-b\epsilon^p}) \quad (5)$$

$$\dot{\alpha} = C \frac{1}{\sigma^0} (\sigma - \phi) \bar{\epsilon}^p - \gamma \phi \bar{\epsilon}^p \quad (6)$$

Here  $\sigma^0$  is the size of the yield surface (size of the elastic range),  $Q_\infty$  (Q infinity) is the maximum increase in the elastic range,  $b$  is a material parameter that defines the rate at which the maximum size is reached as plastic straining develops and  $Y_i$  is the initial yield stress.  $C$  and  $\gamma$  are kinematic hardening parameters, which are material parameters that define the initial hardening modulus and the rate at which the hardening modulus decreases with increasing plastic strain, respectively (Simulia, 2007).

## II. EXPERIMENTAL AND FE ANALYSIS PROCEDURES

The details of the experimental and FE simulations are presented in this section.

### a) Laboratory Reverse Bending, Straightening and Tensile Testing of Wires

A length of the wire was bent and reverse bent round a 100mm diameter cylindrical steel block as shown in Figure 2 and the reverse bent wire was finally straightened and cut into tensile test specimens hereinafter referred to as the experimental reverse bent and straightened (ERBS) wire specimens. The ERBS specimens and tensile specimens cut from the as-received unbent wire specimen hereinafter referred to as unbent wire tensile specimens were tested using an Instron universal testing machine (IX 4505) fitted with an Instron 2518 series load cell with a maximum static capacity of  $\pm 100$  kN. The displacement was measured with an Instron 2630-112 clip-on strain gauge extensometer with a 50 mm gauge length.



Figure 2 : Experimental simulation of reverse bending of wires for civil engineering applications

### b) Reverse Bending, Straightening and Tensile Testing Simulation Procedures

Figure 3 shows the model of a 305m long wire length, the left and right rollers and a guide plate introduced to prevent roller 2 from lifting vertically upward during the bending simulation. The whole model was meshed with C3D8R elements (8-node hexahedral linear brick reduced integration elements with hourglass control). The rollers and the guide plate were meshed with 3mmx3mmx3mm elements. The outer sections of the wire length were meshed with 3mmx3mmx0.5mm elements and the middle 50mm length designated as the FE tensile test specimen was meshed with a finer mesh with 3mmx1mmx0.5mm dimensions. The 3mmx1mmx0.5mm element size was established through mesh convergence studies to be the optimum mesh size required for accurate predictions of the bending and tensile behaviours of the FE tensile test specimen. The 3mm, 1mm and the 0.5mm dimensions are in the FE tensile test specimen's width, length and thickness respectively.

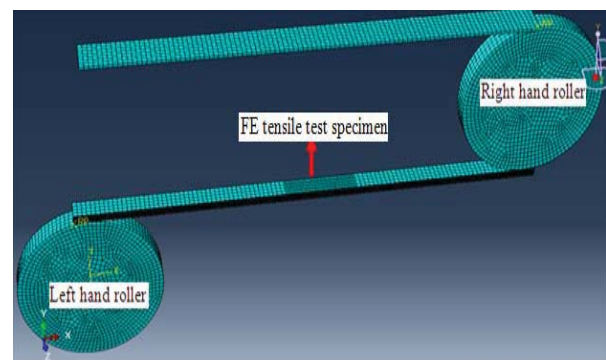


Figure 3 : Meshed model of rollers, guide plate and wire

The left hand roller was rotated in an anticlockwise direction to bend the wire round the left hand roller. After the bending simulation, the left hand roller and the right hand roller were simultaneously rotated in a clock wise and antilock wise directions respectively to unwind the wire from the left hand roller and reverse bend the wire round the right hand roller. After the reverse bending simulation, the right hand roller was rotated in a clockwise direction to unwind the reverse bent wire whilst simultaneously pulling the left hand roller longitudinally and vertically upward until the FE reverse bent test specimen was straightened. The FE reverse bent and straightened wire tensile specimen hereinafter referred to as FERBS was subjected to tensile testing by fixing the left hand end of the specimen and the left hand end of the FERBS tensile specimen, and pulling the right hand end of the specimen and the right hand end of the

FERBS tensile specimen. The right hand end roller; the remaining section of the wire length at the right hand end of the specimen and the right hand end of the FERBS tensile specimen were free to move only in the tensile load direction (i.e. longitudinally in X-axis direction).

The same model arrangement shown in Figure 3 and the same boundary conditions employed for the simulations of the tensile testing of the FERBS wire specimen were employed for the simulations of the tensile testing of the unbent wire except that the bending, reverse bending and straightening simulation steps were suppressed (i.e. not conducted) during the simulations of the tensile testing of the unbent wire.

### c) FE Analysis with isotropic and combined hardening plasticity models

The simulations of the tensile testing of the unbent and FERBS 5x12mm cross section steel wires were conducted with the isotropic and with the combined hardening plasticity models. Both the simulations with the isotropic and with the combined hardening plasticity models were conducted in combination with the phenomenological shears failure model inbuilt in Abaqus. The calibrated shear damage and failure modelling parameters employed for the FE simulations are fracture strain of 0.3451, shear stress ratio of 12.5, strain rate of  $0.000125s^{-1}$  and a material parameter  $K_s$  of 0.3 which were obtained through a phenomenological curve fitting process. Details of the phenomenological curve fitting process employed to obtain the calibrated phenomenological shear failure modelling parameters for the wire considered in this work have been published by Adewole and Bull, (2013).

The material input parameters for the simulation conducted with the isotropic hardening model are the true stress and true strain values obtained from experimental tensile testing of the wires. The true stress and strain values are not presented in this paper for confidentiality purposes (i.e. due to a non-disclosure agreement on the tensile properties of the wires). Other parameters employed for the simulation conducted with the isotropic elastic-plastic model are the density of  $7.6 \times 10^6 \text{ kg/mm}^3$ , Poisson's ratio of 0.3 and Young's modulus of  $200 \times 10^3$ .

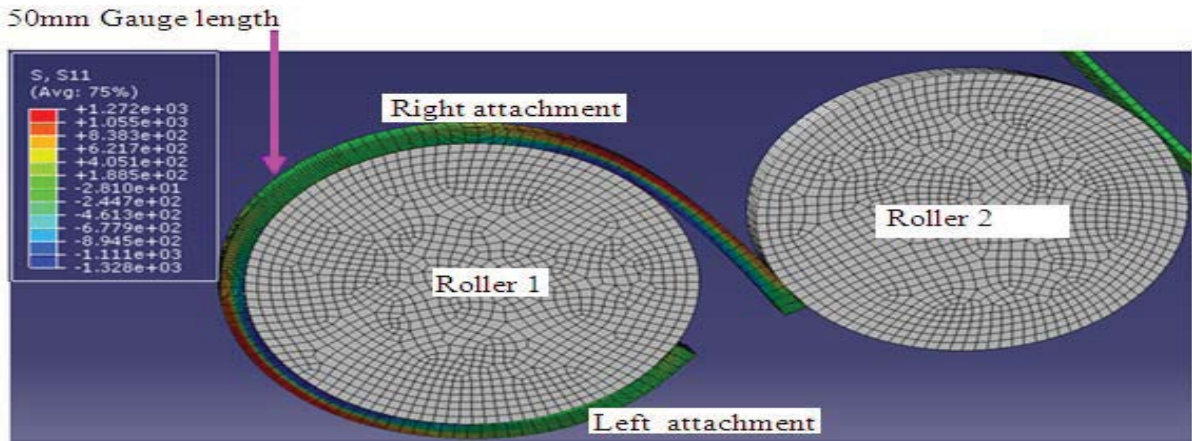
The material input parameters for the simulation conducted with the combined hardening model are the initial stress  $Y_i$  at zero plastic strain (not presented for confidentiality purposes) and the calibrated combined hardening plasticity modelling parameters: kinematic hardening parameter  $C$  of 15300, gamma ( $\gamma$ ) of 275,  $Q_\infty$  of 12000 and hardening parameter  $b$  of 0.04. The calibrated combined hardening plasticity modelling parameters were obtained through a phenomenological curve fitting process and they represent the values of

the modelling parameters at which the FE predicted force-displacement curve agreed with the experimental curve. The phenomenological curve fitting was conducted by carrying out FE simulations of the tensile testing of unbent wire specimens with varying combined hardening modelling parameters until the FE predicted force-displacement curve agreed with the experimental curve up to the fracture initiation point.

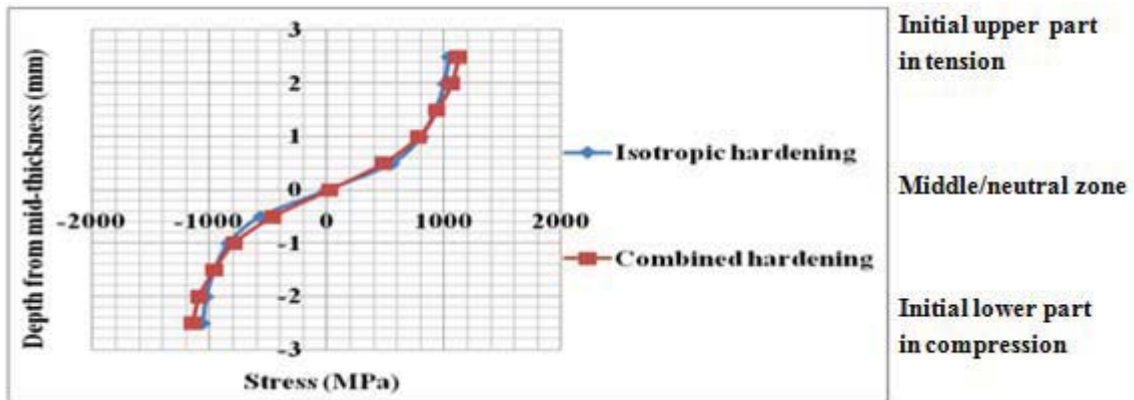
## III. RESULTS

The deformed shapes of the wire showing the longitudinal axial stress ( $S_{11}$ ) distribution and the through-thickness longitudinal axial stress and equivalent plastic strain profiles in the deformed wire specimen at the various stages of the reverse bending and straightening test simulation are presented in this section. In the  $S_{11}$  contour plot, positive axial stresses represent tensile axial stresses and the negative axial stresses represent compressive axial stresses. The deepest red colour at the top of the contour plot represents the highest tensile stress while the deepest blue at the bottom of the contour plot represents the highest compressive stress. For both the through-thickness longitudinal axial stress and the through-thickness equivalent plastic strain profiles, positive and negative stresses and strains represent tensile and compressive stresses and strains respectively. The stress and strain in the upper half thickness and the lower half thickness of the 5mm thick wire are plotted with 0 to 2.5mm and 0 to -2.5mm Y-axis coordinates respectively.

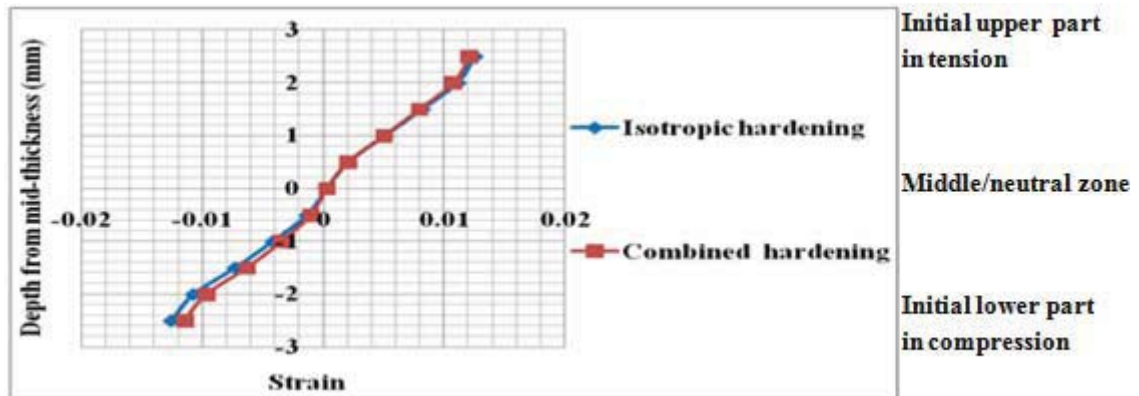
Throughout the bending, reverse bending, straightening and tensile testing simulations, the deformed shapes predicted by the simulations conducted with the isotropic hardening and with the combined hardening models are exactly the same. Consequently, only the deformed shapes predicted by the simulation conducted with the combined hardening models after the bending simulation, during the reverse bending simulation, after the reverse bending simulation, after the straightening simulation and after the tensile testing simulation are presented in Figures 4, 5, 6, 7 and 8 respectively. The through-thickness longitudinal axial stress and equivalent plastic strain profiles in the bent, reverse bent, and reverse bent and straightened wire specimens predicted by the simulations with the two hardening models are also presented in Figures 4, 6 and 7 respectively. The fractured experimental ERBS wire specimen is shown in Figure 8(c). The experimental force-displacement curves for the unbent and ERBS wire specimens with the force-displacement curves obtained from the simulations of the tensile testing of the unbent and FERBS wire specimens conducted with the isotropic and the combined hardening plasticity models are shown in Figures 9 and 10 respectively.



(a) Deformed shape showing longitudinal axial stress distribution



(b) Through-thickness longitudinal axial stress profile



(c) Through-thickness longitudinal axial plastic strain profile

Figure 4 : Longitudinal axial stress and equivalent plastic strain distributions and through-thickness profiles in wire after bending process simulation

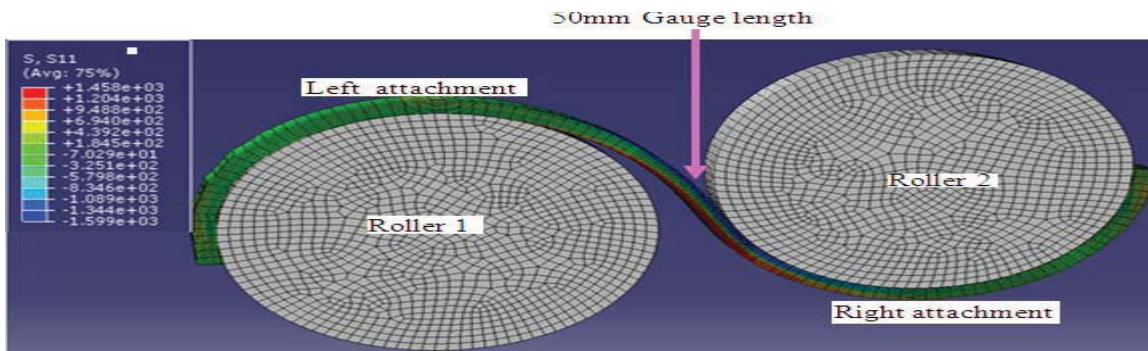
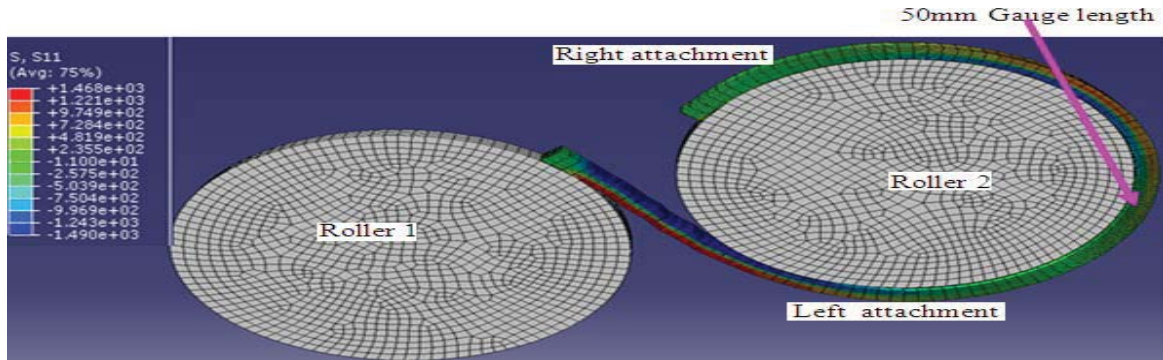
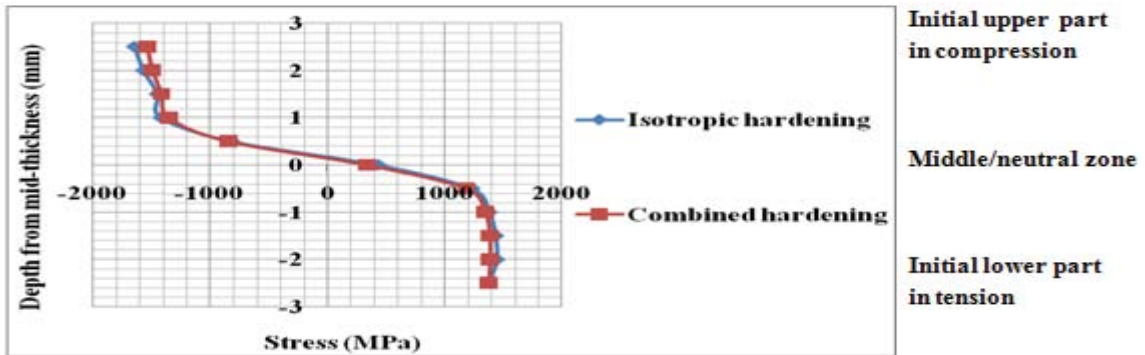


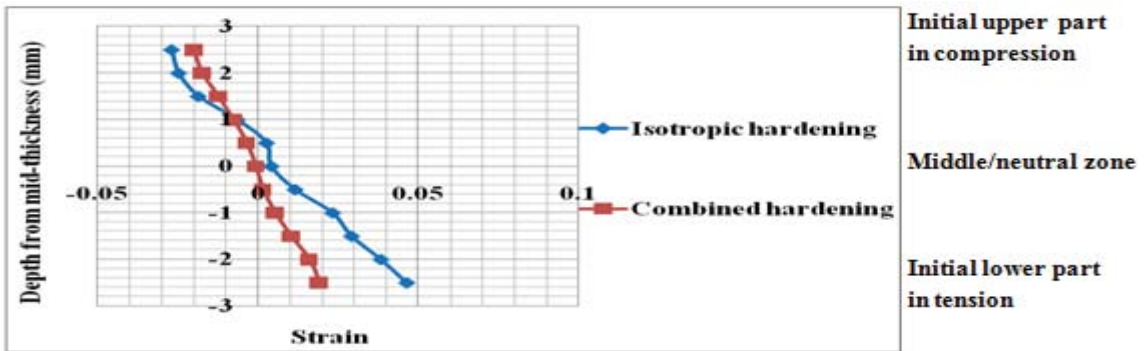
Figure 5 : Deformed shape showing longitudinal axial stress distribution in specimen during reverse bending process simulation



(a) Longitudinal axial stress distribution in whole wire length

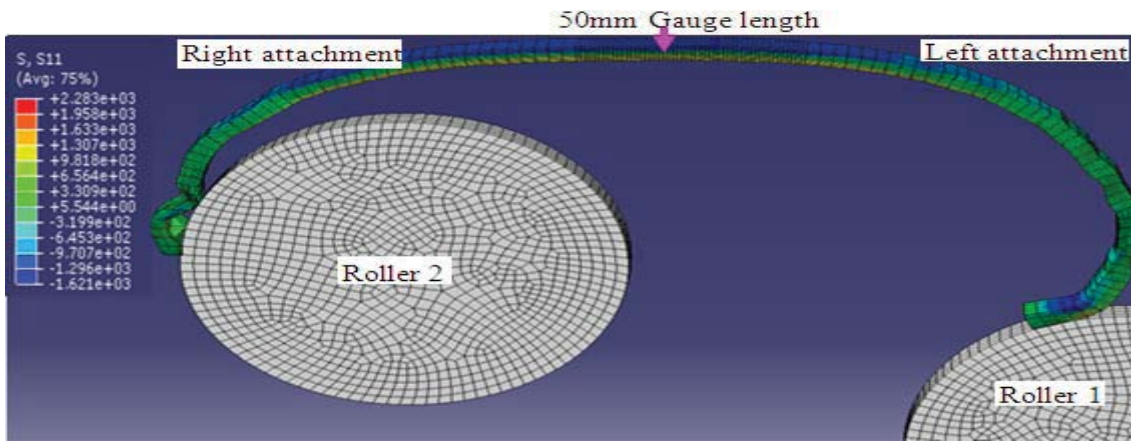


(b) Through-thickness axial stress profile

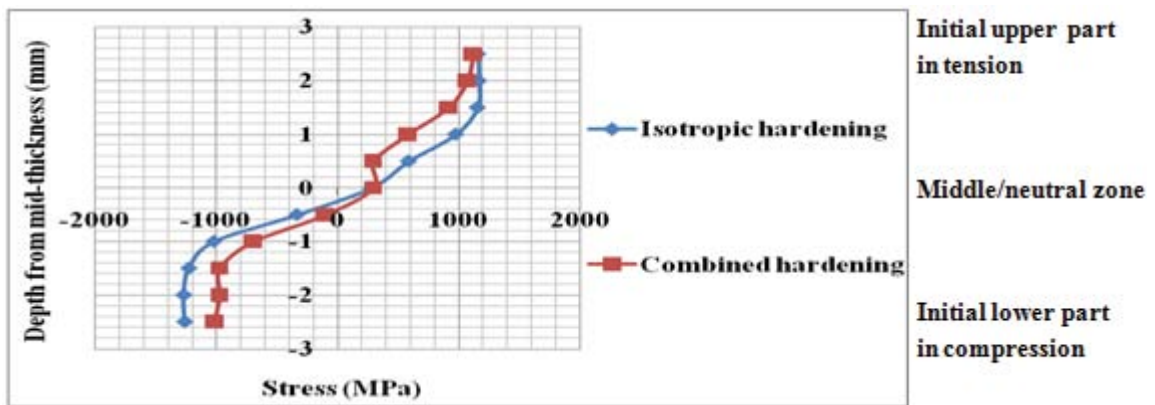


(c) Through-thickness axial plastic strain profile

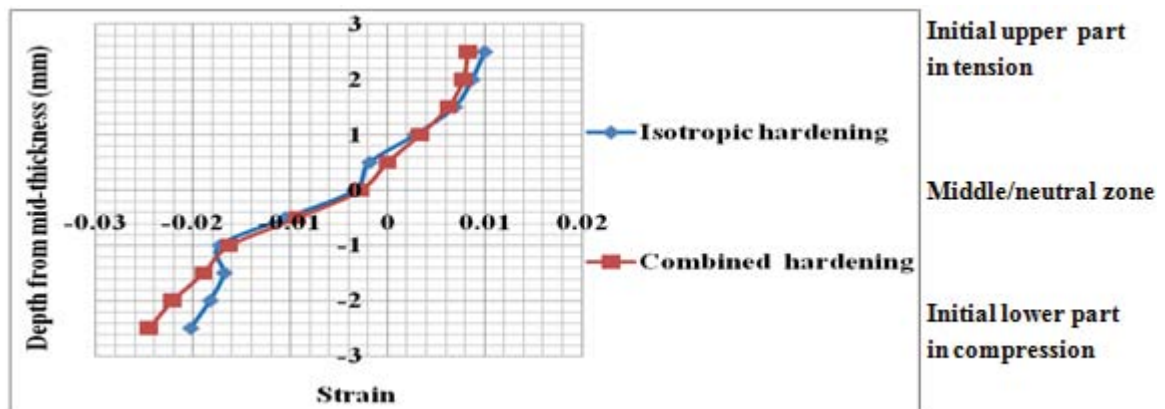
Figure 6 : Longitudinal axial stress and equivalent plastic strain distributions and through-thickness profiles in wire after reverse bending process simulation



(a) Deformed shape and stress distribution in whole wire length

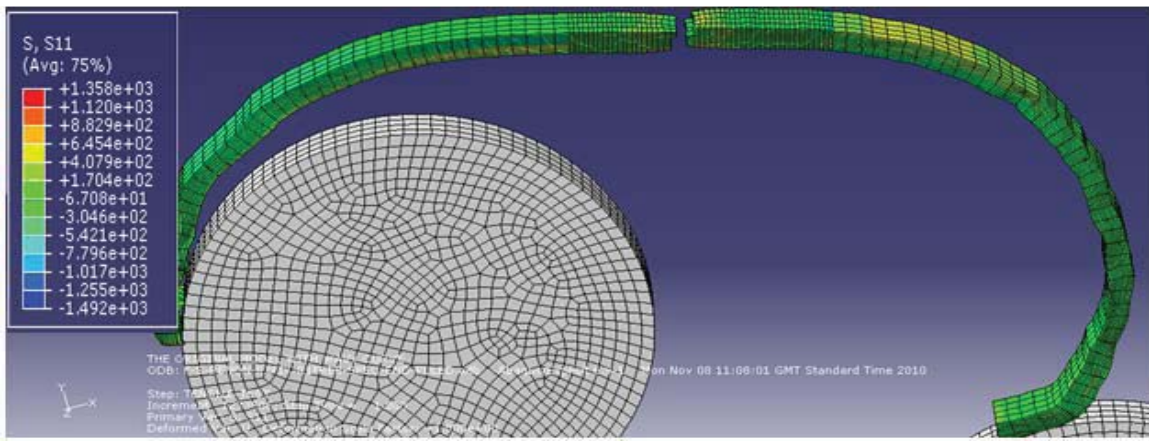


(b) Through thickness longitudinal axial stress profile

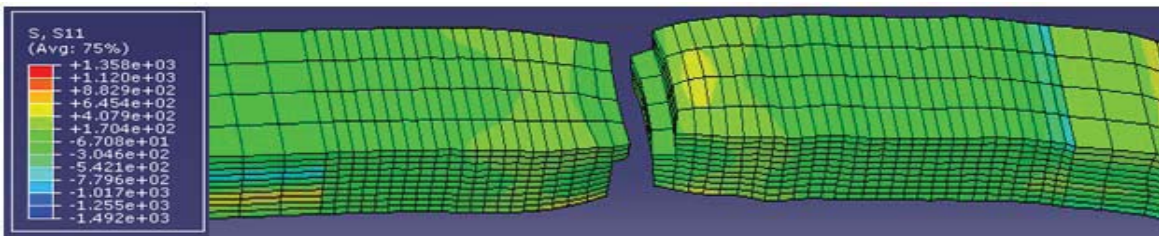


(c) Through-thickness axial plastic strain profile

Figure 7 : Longitudinal axial stress and equivalent plastic strain distributions and through-thickness profiles in wire after straightening process simulation



(a) Deformed shape of the whole wire length showing the Fractured FERBS specimen at the center of the whole wire length



(b) Fractured numerically RBS specimen alone



(c) Fractured experimentally RBS specimen

Figure 8 : Fractured numerically and experimentally RBS specimens after tensile testing

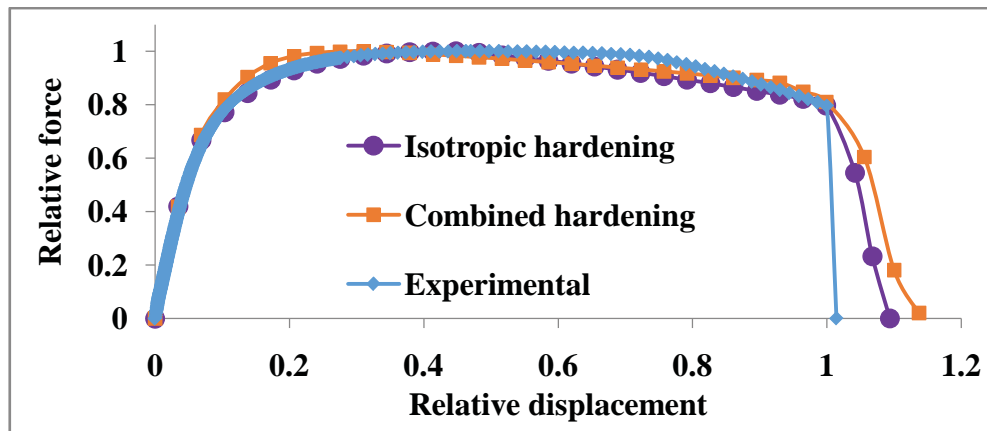


Figure 9 . Experimental and FE force-displacement curves for unbent wire specimens with isotropic and combined hardening models

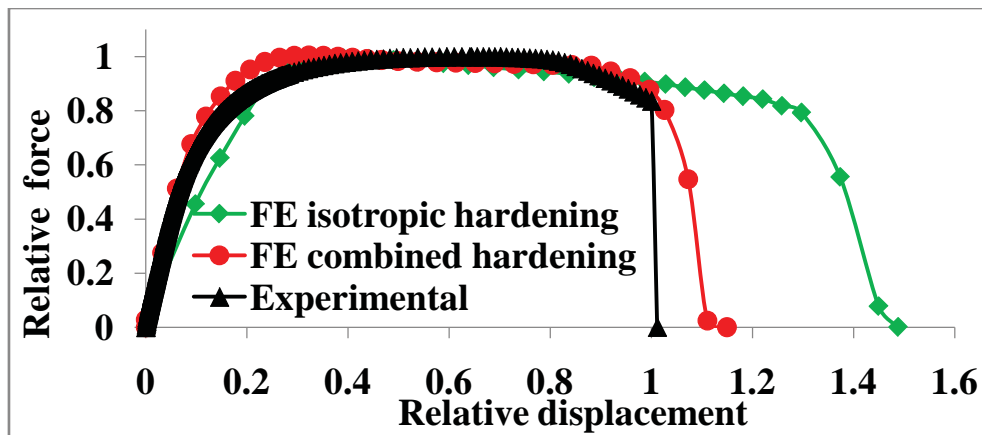


Figure 10 : Experimental and FE force-displacement curves for RBS wire specimens with isotropic and combined hardening models

## XI. DISCUSSION

As shown in Figures 4(b) and (c), there is no significant difference in the through-thickness longitudinal axial stresses and strains profiles predicted by the bending simulations conducted with both the isotropic and the combined hardening models. The simulations conducted with both hardening models predicted tensile and compressive stresses and strains at the initial upper and the initial lower parts of the wire as expected based on the deformed shape of the wire specimen shown in Figure 4(a). Also the strain profiles predicted by the simulations conducted with the two hardening models are linear as expected of a bending induced straining. This result indicates that both the isotropic and the combined hardening models are able to predict the stress and strain distributions/profiles in wires subjected to bending round the roller accurately.

Similarly, there is no significant difference in the through-thickness longitudinal axial stress profiles predicted by the reverse bending simulations conducted with both the isotropic and the combined hardening models as shown in Figures 6(b). Also the simulations conducted with the two hardening models predicted the expected strain reversal in the reverse bent wire specimen as the initial upper and initial lower parts of the wire that were subjected to tensile and compressive stresses after the bending simulation are now subjected to compressive and tensile stresses and strains respectively after the reverse bending simulation. However, the strain profile predicted by the simulation conducted with the combined hardening model is linear as expected for a bending induced straining, whereas the strain profile predicted by the simulation with the isotropic hardening model is not linear. Now, a difference between the capability/suitability of the isotropic hardening model and the combined hardening model in predicting the appropriate/expected linear strain profile in the reverse bent wire specimen that has undergone strain reversal is observed.

The straightening of the wire caused a second stress and strain reversal and induced tensile and compressive stresses and strains in the initial upper and initial lower parts of the wire specimens respectively as shown in Figure 7(a). Consequently, the initial upper part of the wire specimen has undergone a “double” stress/strain reversal resulting from the tensile stress/strain in the upper part of the wire due to bending, followed by compressive stress/strain in the upper part of the wire due to the reverse bending and followed by the tensile stress in the upper part of the wire due to straightening of the wire. Similarly the initial lower part of the wire has undergone a double strain reversal (compressive stress due to bending, tensile stress due to reverse bending and compressive stress due to straightening). There is a significant difference in the through-thickness longitudinal axial stress profiles predicted by the simulations conducted with the isotropic model and with those conducted with the combined hardening model as shown in Figure 7(b), with the simulation conducted with the isotropic hardening model predicting higher tensile and compressive stresses at the upper and the lower parts of the wire respectively. The strain profiles predicted by the two hardening models shown in Figure 5(c) are no longer linear due to the plastic straining involved in the straightening process.

The simulations of the tensile testing of the FERBS specimen conducted with the two hardening models predicted the same fracture shape shown in Figure 8(b), which agrees well with the fracture shape exhibited by the experimentally RBS specimen shown in Figure 8(c). This result indicates that the fracture process and the predicted fracture shape are largely independent of the hardening model and solely dependent on the phenomenological shear fracture model employed for the simulations with the two hardening models.

Figure 9 indicates that the force-displacement curve predicted by the simulations of the tensile testing of the unbent wire with both isotropic and combined

hardening models agree well with the experimental curve up to the fracture initiation point. The force-displacement curve predicted by the simulation of the tensile testing of the FERBS wire with the combined hardening model agrees very well with the experimental curve throughout the elastic region, and fairly well in the plastic and fracture regions (Figure 10). However, the force-displacement curve predicted by the simulation of the tensile testing of the FERBS with isotropic hardening does not show a good agreement with the experimental curve throughout the elastic region.

It is considered that the difference between prediction and experiment is due to the fact that the isotropic hardening model does not capture the softening of the wire due to the Bauschinger effect and merely predicts that the wire has been continuously work hardened during the bending, reverse bending, and straightening operations, which is not evident in the experimental curve. The inability of the isotropic hardening model to capture the softening of the wire due to the Bauschinger effect associated with the double strain reversal involved during the reverse bending and straightening simulation also explains why the simulation conducted with the isotropic hardening model predicted higher through-thickness stress values as shown in the stress profile of the FERBS wire in Figure 7(b). Conversely, the combined hardening model adequately captured both the work hardening and Bauschinger effect that are associated with the double strain reversal involved in the reverse bending and straightening processes. Figure 10 also indicates that the isotropic hardening model predicts a displacement at fracture far higher than the experimental results. Consequently, it is concluded that the combined hardening model is the appropriate material constitutive (plasticity hardening) model for the simulation of bending, reverse bending, and straightening of carbon steel wires used for civil engineering applications.

## XII. CONCLUSION

In this paper, it is demonstrated that both the isotropic and the combined hardening models are able to predict the bending behaviour of wires for civil engineering applications as they both predicted the stress and strain distributions and profiles in bent wire accurately. However, the isotropic hardening model does not give good predictions of the stress and strain distributions and profiles, and also does not give a good prediction of the tensile behaviour of the reverse bent and straightened wire which has undergone “double strain reversal” due to the reverse bending and straightening operations. This is due to the fact that the simulation conducted with the isotropic hardening model predicted a continuous work hardening of the wire during the bending, reverse bending, and straightening operations and did not capture the softening of the wire due to the Bauschinger effect that

is associated with the double strain reversal experienced by the reverse bent and straightened wire. Conversely, the simulation conducted with the combined hardening model adequately captured both the work hardening due to bending and the softening of the wire due to the Bauschinger effect resulting from the “double” strain reversal experienced by the wire during reverse bending and straightening operations. Consequently, it is concluded that the combined hardening model serves as the most appropriate plasticity hardening model for the prediction of the behaviour of carbon steel wires subjected to bending, reverse bending, and straightening.

This work thus identifies the combined hardening model as the appropriate plasticity hardening model for wires for civil engineering applications reverse bending and straightening test simulation. This work thus provides the appropriate material constitutive model required for the numerical simulation of wires reverse bending and straightening test which is required for the numerical investigation of the effects of the combination of reverse bending and laminations on the tensile properties of a typical wire used for civil engineering applications which cannot be done experimentally as it is impossible to machine the long straight longitudinal laminations into the wires.

## REFERENCES RÉFÉRENCES REFERENCIAS

1. Adewole K. K, Bull S. J., 2013. Prediction of the fracture performance of defect-free steel bars for civil engineering applications using finite element simulation. *Construction and Building Materials*, Volume 41, pages 9–14.
2. Carbonnie J Thuillier., S, Sabourin F., Brunet, M and Manach P.Y., 2008. Comparison of the work hardening of metallic sheets in bending–unbending and simple shear. *International Journal of Mechanical Sciences*, Vol 51, pages 122–130.
3. Firat M., 2007. U-channel forming analysis with an emphasis on springback deformation. *Materials and Design*, Volume 28, pages 147–154.
4. Gau Jenn-Terng and Kinzel Gary L., 2001. A new model for springback prediction in which the Bauschinger effect is considered. *International Journal of Mechanical Sciences*, 2001, Vol 43, Issue 8, Pages 1813-1832.
5. Hooputra, H., Gese, H., Dell, H., and Werner, H., 2004. A Comprehensive Failure Model for Crash worthiness Simulation of Aluminium Extrusions. *International Journal of Crashworthiness*, Vol. 9, no.5, Pages 449–464.
6. Ken-ichiro, Mori., 2001. Simulation of materials processing: theory, methods and applications: proceedings of the 7th International Conference on Numerical Methods in Industrial Forming Processes

- NUMIFORM 2001, pages 711-721. Paper presented by Cedric Xia, Z.
7. Simulia, 2007. Abaqus documentation, Abaqus Incorporated, Dassault Systemes.
  8. Smith B.O., Jenning A.P.H and Grimshaw A.G., 1957. A portable lamination detector for steel sheet, The British Iron and Steel Research Association, Battersea Park Road, London.
  9. Taherizadeh, Aboozar., Green, Daniel E., Ghaei, Abbas and Jeong-Whan Yoon, 2010. A non-associated constitutive model with mixed isokinematic hardening for finite element simulation of sheet metal forming. International Journal of Plasticity, Vol 26, pages 288–309.
  10. Takeda, T. and Chen Z., 1999. Yield Behaviour of Mild Steel after Prestraining and Aging under Reversed Stress. Metallurgical and Materials Transactions A, Vol 30A, pages 411-416.
  11. United States Bureau of Reclamation, "Prestressed Concrete Pipe Failure Jordan Aqueduct, Reach 3" (1994). All U.S. Government Documents (Utah Regional Depository). Paper 284.<http://digitalcommons.usu.edu/govdocs/284>, assessed on 15/11/2012.
  12. Zhao K.M. and Lee J.K.,1999. On simulation of bend/reverse bend of sheet metals American ciety of Mechanical Engineers, Manufacturing Engineering Division, MED Volume 10, 1999, Pages 929-933.



This page is intentionally left blank